Available online at www.sciencedirect.com
SCIENCE DIRECT®
Journal of Power Sources 145 (2005) 169–177
JOURNAL OF POWER SOURCES
www.elsevier.com/locate/jpowsour

Experimental investigation of anodic gaseous concentration of a practical seal-less solid oxide fuel cell

Akihiko Momma [a,*], Yasuo Kaga [a], Kiyonami Takano [a], Ken Nozaki [a], Akira Negishi [a], Ken Kato [a], Tohru Kato [a], Toru Inagaki [b], Hiroyuki Yoshida [b], Koji Hoshino [c], Masaharu Yamada [c], Taner Akbay [c], Jun Akikusa [c]

[a] *Fuel Cell Group, Energy Technology Research Institute, National Institute of Advanced Industrial Science and Technology, Tsukuba Central #2, 1-1-1 Umezono, Tsukuba-shi, Ibaraki 305-8568, Japan*
[b] *Energy Use R&D Center, The Kansai Electric Power Company Inc., 11-20 Nakoji, 3-Chome, Amagasaki, Hyogo 661-0974, Japan*
[c] *Central Research Institute, Naka Research Center, Mitsubishi Materials Corp., 1002-14 Mukohyama, Naka-machi, Naka-gun, Ibaraki 311-0102, Japan*

Accepted 30 December 2004
Available online 13 April 2005

Abstract

In order to verify the validity of the simulation and to investigate the gaseous diffusion from the outlet of the anode, anodic gas concentration measurements of a seal-less disk-type solid oxide fuel cell (SOFC) were carried out using quadrupole mass spectrometer (QMS). Simultaneous gas sampling was conducted from the five sampling ports made at the anode separator. The uniformity of the radial gas flow in the anode was confirmed by analyzing the gas from four sampling ports located at a concentric circle. H_2, H_2O and N_2 concentration profiles were measured and simulated under various fuel utilization (U_f) conditions and changing the gas flow rate. The diffusion of N_2 into the anode was found to become less with increasing U_f owing to the lesser diffusivity of N_2 in H_2O than in H_2. From the simulation, the existence of the reverse current, i.e., electrolysis current, in the outlet region was predicted. It was confirmed that the existence of the electrolysis current is possible by measuring the concentration of the gas in the anode under electrolysis operations. The comparison of *V–i* characteristics measured and simulated revealed that the effect of the concentration polarization is not significant and suggested the validity of the assumption made for the simulation.

Keywords: Solid oxide fuel cell; Gas concentration measurement; Concentration profile; Steam electrolysis; Simulation; Mass spectrometry

1. Introduction

Fuel cell is a prospective power generation method in terms of its cleanness and high efficiency. Solid oxide fuel cell (SOFC), especially, has a possibility of the highest efficiency when incorporated into co-generation or combined system and of correspondence to various fuels [1,2] and it is expected to be one of the most promising electric power generation technologies in the coming energy saving world [3]. In order to use SOFC widely, the basic research to establish the evaluation standard to support the enhancement of the commercialization are still needed including the precise understanding of its characteristics.

During the last few years, we have been working for the simulation of the characteristic behavior of practical single cell SOFC and for the impedance measurement [4,5] using SOFC based on lanthanum gallate developed by Mitsubishi Material Corp. [6,7]. The cell used for the impedance measurements here works at around 1023 K, and has seal-less structure [6].

In order to understand the behavior of SOFC, the precise knowledge about the gaseous concentration in the cell is essential. For instance, we have already shown [4,5,8,9] that the

* Corresponding author. Tel.: +81 29 861 5735; fax: +81 29 861 5805.
E-mail address: mo.momma@aist.go.jp (A. Momma).

0378-7753/$ – see front matter © 2005 Elsevier B.V. All rights reserved.
doi:10.1016/j.jpowsour.2004.12.062

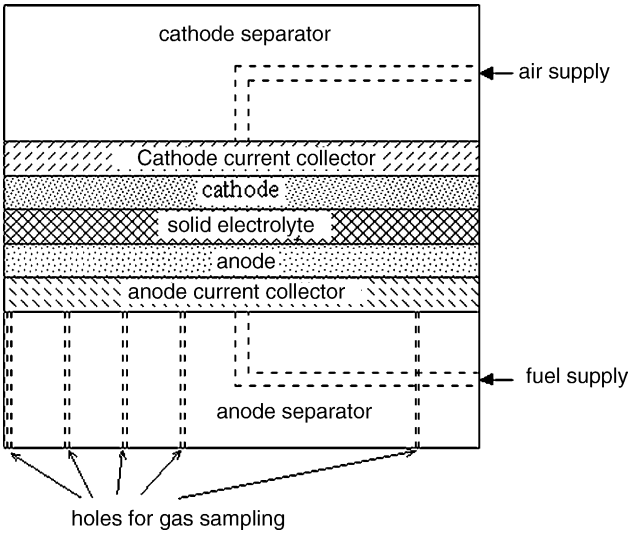

Fig. 1. Schematic cross-section of the single cell setup.

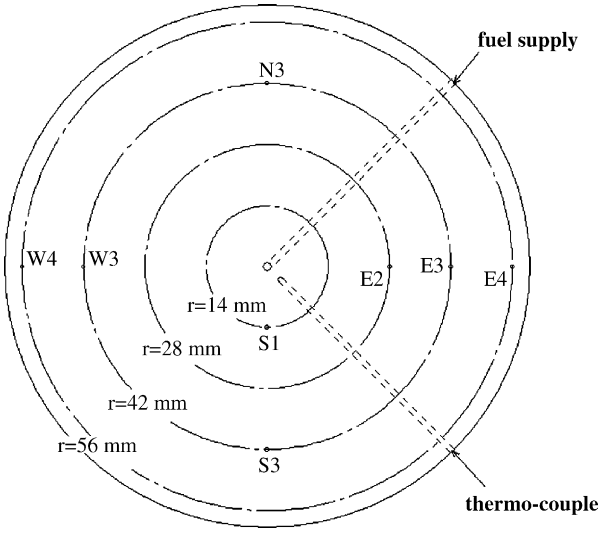

Fig. 2. Top view of the anode separator prepared for the gas sampling.

behavior of the practical cell is dominated by the impedance which originates from the change of electro-motive force (emf), i.e., the knowledge about the gaseous concentration in the cell offers a key information of SOFC behaviors under practical operations.

One of the complexities that make the situation difficult to simulate is the existence of the electronic conduction in the electrolyte, which gives rise to the local internal current. Another complexity comes from the seal-less structure. The diffusion of the ambient air into the anode from the seal-less edge can be considered to occur quite naturally. However, it is very hard to take the effect of the diffusion into simulation with proper boundary conditions without any experimental evidence.

Although in our simulation, which has been presented so far [4], the back diffusion of the ambient air through the seal-

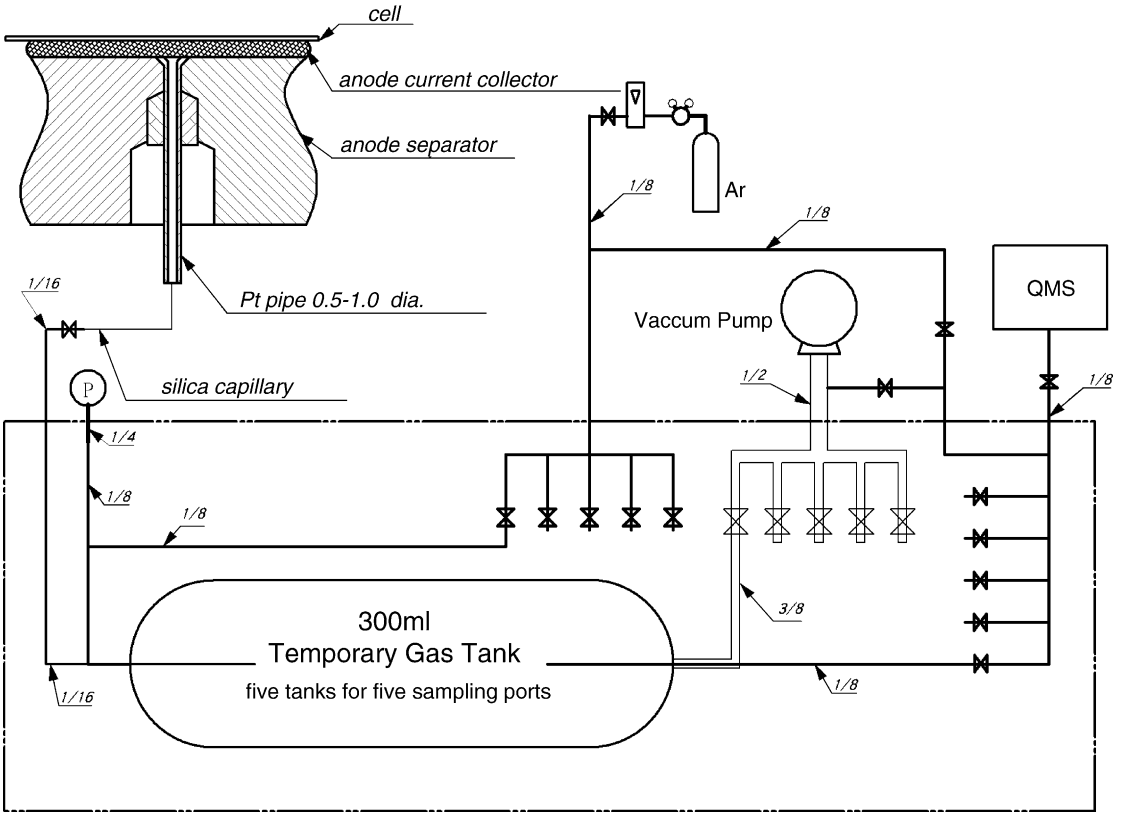

Fig. 3. The gas sampling system built to work for the simultaneous sampling from five sampling ports.

less outermost edge was not taken into account and the electronic transference number in the electrolyte was assumed to be uniform, the characteristic behavior of the cell was reasonably explained to some extent with some discrepancies between the simulation and the experiment remaining unexplained. Consequently, the necessity of the more accurate simulation has been suggested [9].

The objective of the present work is to verify the following matters:

(1) validity of the simulation including the uniformity of the radial gas flow;
(2) the amount of the gasses that diffuse into the anode from the seal-less edge;
(3) Confirmation of (1) establishes the validity of the assumption, while (2) provides the basic data for more accurate simulations.

In the following simulations, the electronic transference number in the electrolyte was still assumed to be uniform throughout the cell because it would require more accurate and systematic analyses of the gaseous composition. The effect of the back diffusion was taken into account in the simulation and the discussion was made by comparing the measured data and the simulation.

2. Experimental

2.1. Single cell and its setup

Experimental cell setup is shown in Fig. 1. Single cell (120 mm diameter) made of lanthanum gallate $La_{0.8}Sr_{0.2}Ga_{0.8}Mg_{0.15}Co_{0.05}O_{3-\delta}$ as solid electrolyte (ca. 0.2 mm thickness), $Sm_{0.5}Sr_{0.5}CoO_3$ as cathode, $Ni/Ce_{0.8}Sm_{0.2}O_{1.9}$ cermet as anode is placed between cathode and anode separators with structured current collectors between the electrode and the corresponding separator.

Hydrogen is used for the anode gas at the flow rate of 340 Ncc min^{-1} and air for the cathode at 1700 Ncc min^{-1}, unless otherwise noted. These gas flow rates together with the current of 34 A (average current density of 0.3 A cm^{-2}, U_f = 70%) were chosen as the standard condition considering the practical applications. Each gas is supplied through the holes made at the center of the separator to each electrode and radially flown through the structured-current collectors to the outermost seal-less edge of the cell where they spread to the ambient atmosphere.

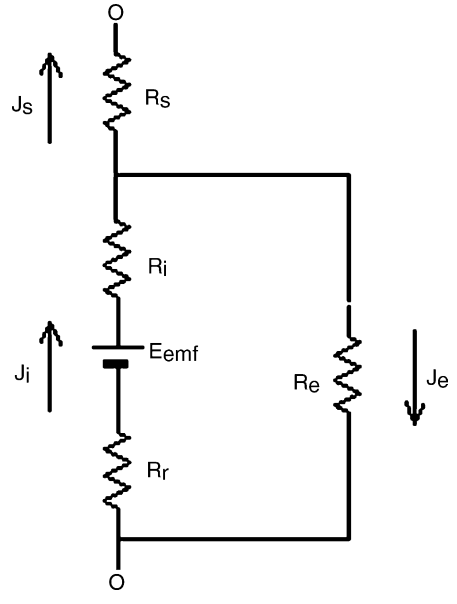

Fig. 4. Equivalent circuit assumed for the simulations.

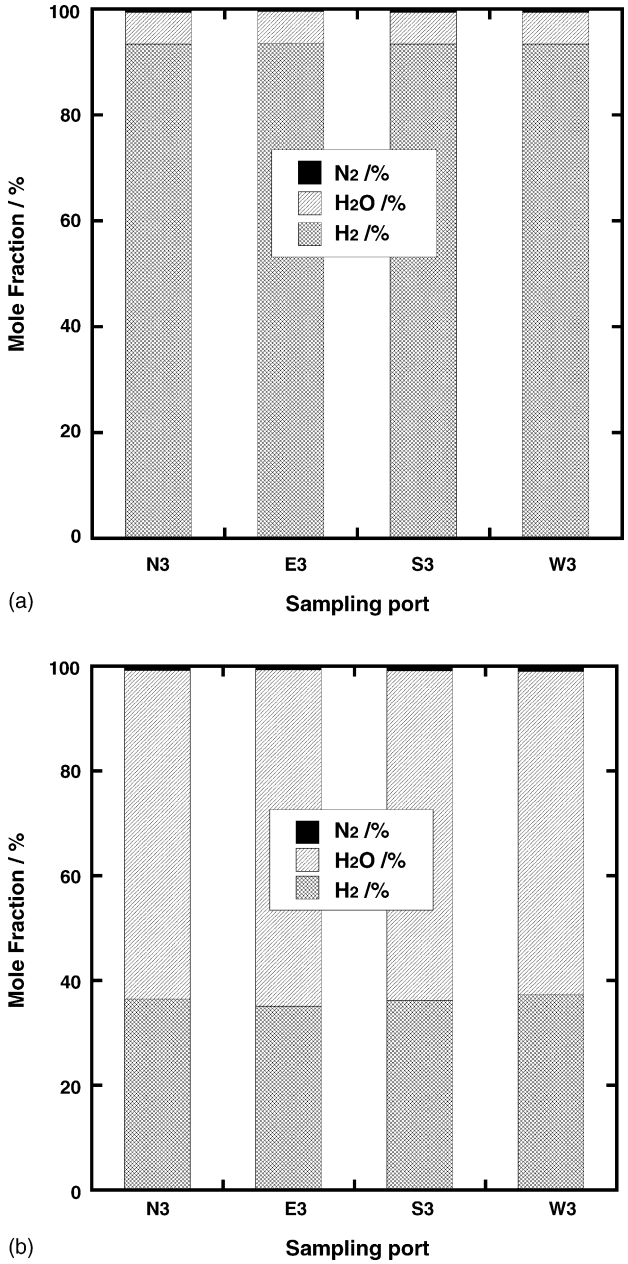

Fig. 5. Measured mole fraction of H_2, H_2O and N_2 of the gasses sampled from the 4 sampling ports located at r = 42 mm (N3, E3, S3 and W3 in Fig. 2): (a) U_f = 0% and (b) U_f = 70%.

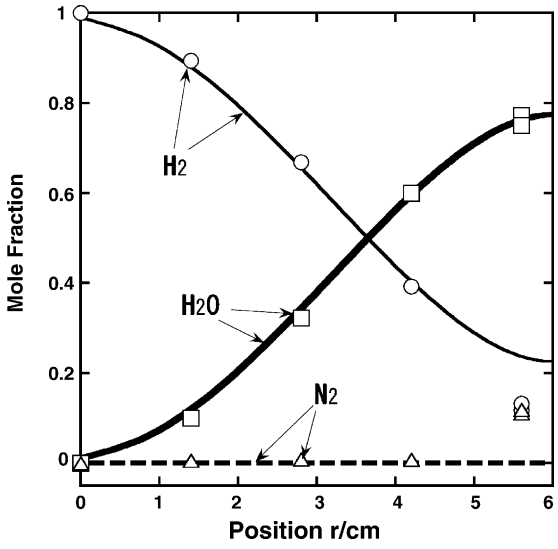

Fig. 6. Measured concentration (symbols) of H_2, H_2O and N_2 with the simulated profiles without considering the back diffusion.

The dc current was supplied by potentio-galvanostat (Nikkoukeisoku NPGS-10-100). The ac impedance measurements, which were conducted to measure the characteristic behavior of the cell under electrolysis direction in this work, were carried out in the same manner as described elsewhere [9]. Steam was also provided together with hydrogen in the electrolysis experiments. The experimental procedure for steam supply is also described in the literature [9].

2.2. Gas sampling and introducing to the analyzer

Anode gasses are sampled through the sampling ports, which are fabricated by making holes in the anode separator (Fig. 2). The holes were located considering the unaffected location of the gas sampling in the upper stream regions. Suitably selected five sampling ports are connected to silica capillaries at the backside of the separator via platinum tubes (0.5 mm inner diameter). These capillaries are then connected to 1/16 in. stainless steal tubes through which sampled gasses

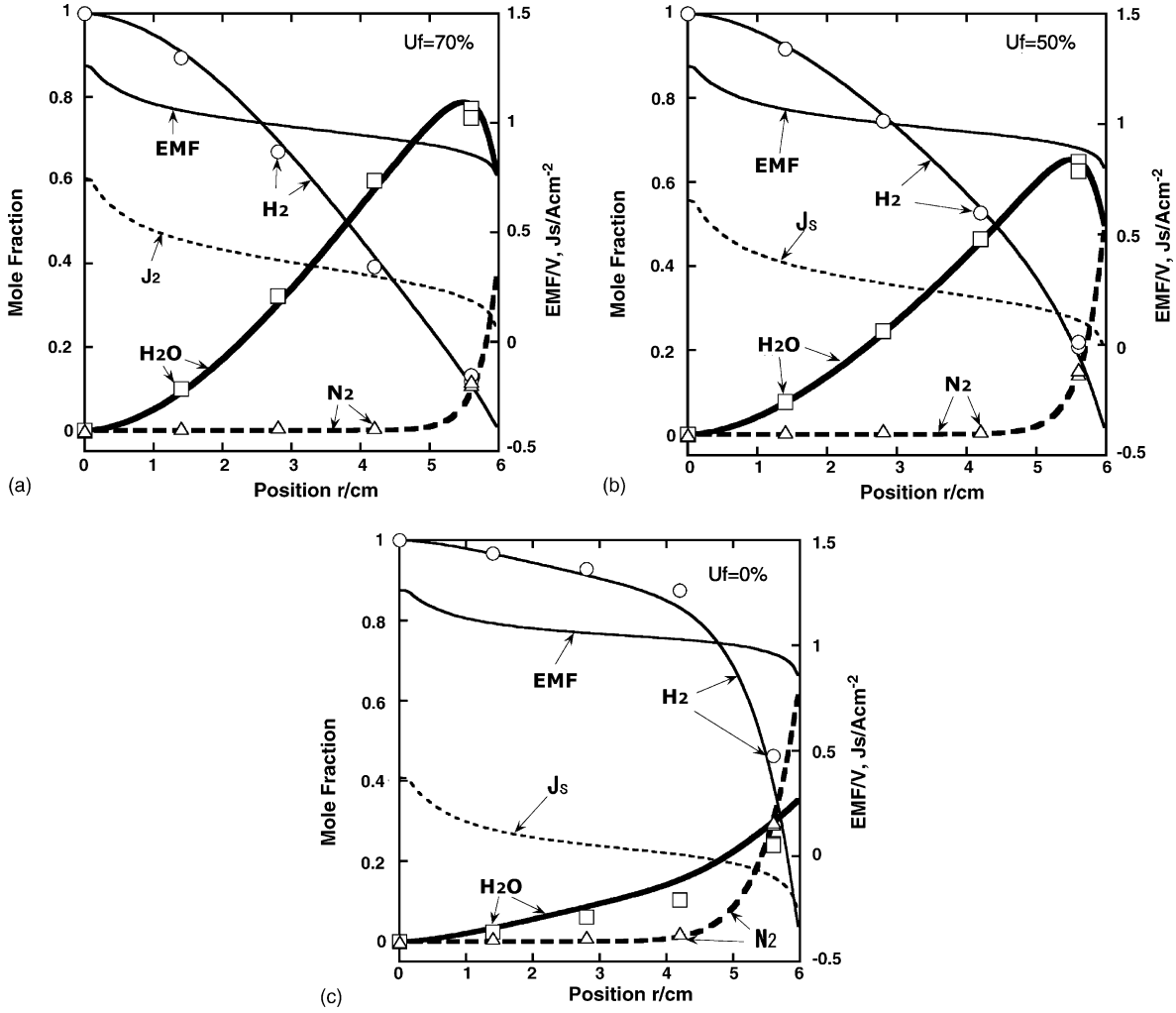

Fig. 7. Measured concentration (symbols) of H_2, H_2O and N_2 with the simulated concentration, emf and J_s profiles considering the back diffusion under: (a) $U_f = 70\%$, (b) $U_f = 50\%$ and (c) $U_f = 0\%$. 1023 K, H_2: 340 Ncc min^{-1}, air: 1700 Ncc min^{-1}.

are sucked into initially evacuated tanks (300 cc) for the temporary storage. In order to minimize the effect of the residual gasses remaining in the tubing, the diameters of these tubing were made as thin as possible. Moreover, the inside surface of the most of the tubing and the tanks are coated by silica. Also, in order to avoid the condensation of steam, the sampling lines are heated and the tanks are kept in a thermostatic oven (surrounded area by alternate long and two short dashes line in Fig. 3).

The pressures in the tanks are monitored by high temperature pressure gauges and the sampling of the gasses is conducted until the pressure in the tanks becomes 0.1 atm. By controlling the valves, this sampling was conducted slowly enough in order that it may not affect the flow condition of the gas in the anode. Argon was then introduced into the tanks and the sampled gasses were pressurized until the pressure became ca. 3 atm. Therefore, the sampled gasses were diluted to ca. 1/30 by Ar.

Finally, the pressurized gasses were sequentially introduced into QMS (ANELVA M-200GA-DM) and were analyzed.

2.3. Calibration of QMS and the data treatment

Prior to the experiments calibration curves of ion current versus gaseous concentration are obtained under simulated conditions using not only single gas diluted by Ar but also the mixture of the two associated gasses diluted by Ar, investigating the effect of the interaction between the different gaseous species. H_2, H_2O, N_2 and O_2 were considered to be included in the anode gas, and the ion current peaks corresponding to mass number of 2, 18, 28 and 32 were investigated. Good linearity between the gaseous concentration and the intensity of the ion current was observed with all the gasses investigated.

Because of the aging of the secondary electron multiplier of QMS, the variation in its gain could not be neglected. Hence, the obtained current peak data were analyzed under the assumption that the relative sensitivities of subject ions do not change. Under the assumption, the relative intensity of mass number 2, 18, 28, 32 and 44 ion currents were used for the calculation of the concentrations of H_2, H_2O, N_2, O_2 and CO_2, respectively. Owing to the effect of the variation of the baseline and the calibration errors, the errors included in the obtained concentration can be estimated to be 1–2%.

3. Calculation

Simulation model and the calculation method are described elsewhere [4]. However, in the former simulation the diffusion of air into the anode was not considered. In this paper, as has been mentioned, the back diffusion of the air into the anode was also considered assuming that the output hydrogen is completely reacted with oxygen from the air to form steam. In the simulation, we assume that this oxidation reaction takes place at the very outlet of the anode ($r = 60$ mm).

In the series of experiments, the maximum concentration of oxygen obtained was 0.07% and no significant CO_2 was observed. Hence, in the simulation, it was assumed that only N_2, H_2 and H_2O exist in the anode.

The equivalent circuit used for the calculation is shown in Fig. 4. Because only dc characteristics are discussed in this paper, no capacitive elements were taken into account. In the figure, R_i represents a resistance of solid electrolyte, R_r represents the resistance for the electrochemical reaction and R_s represents resistances incorporated in the cell in series like contact resistances, material resistances, etc. In the calculation, the values obtained from the ac impedance measurements reported earlier were used and R_i was set to be 0.2 $\Omega\,cm^2$ at 1023 K considering the conductivity of the solid electrolyte [7] and its thickness.

As for the direction of the current in Fig. 4, when locally considered, plus figure of J_s means that the local cell is under fuel cell operation and minus figure of J_s means that the local cell is under electrolysis operation.

4. Results and discussion

4.1. Confirmation of the uniformity of gaseous flow

In Fig. 5, measured concentration of the gasses sampled from four sampling ports (N3, E3, S3 and W3) located at an identical concentric circle ($r = 42$ mm) is shown under an open circuit condition (a) and $U_f = 70\%$ (b). Under the two conditions investigated, no significant variations in the gaseous composition were observed. Because in our simula-

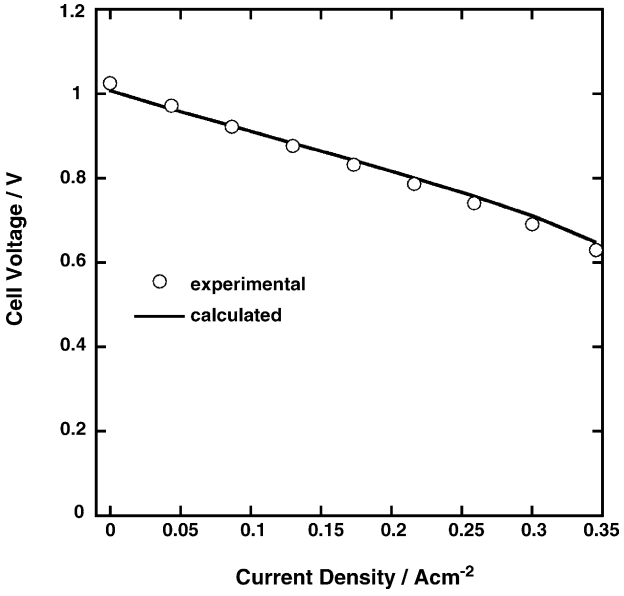

Fig. 8. Comparison of the measured and the calculated *V–i* curves at the standard condition. 1023 K, H_2: 340 Ncc min^{-1}, air: 1700 Ncc min^{-1}.

tion, the uniformity of gaseous flow is assumed, this observation is a strong evidence of the validity of the assumption considering the experimental error (1–2%) included in the measurement.

4.2. Compositional measurement and simulation under standard flow rate

The measured compositional distributions are plotted with the simulated curves obtained without considering the back diffusion at $U_f = 70\%$ condition in Fig. 6. The gasses are sampled from the five sampling ports shown in Fig. 2, i.e., S1, E2, N3, W4 and E4. Two sampled gasses were analyzed from $r = 56$ mm. The points at $r = 0$ are plotted as the composition of the supplied gas. The comparison of the observed data and the simulation reveals the obvious discrepancy at the outlet region, apparently owing to the effect of the back diffusion of N_2. Hence, it was clarified that the consideration of the back diffusion is essential at least under the standard gas flow rate conditions.

The measured data are then plotted with the simulated curves considering the effect of the back diffusion in Fig. 7(a) $U_f = 70\%$, (b) $U_f = 50\%$ and (c) at OCV. As has been noted, for the boundary condition, the complete oxidation of H_2 at $r = 60$ mm is assumed. Considerably good agreement between the experimental data and the simulation is depicted

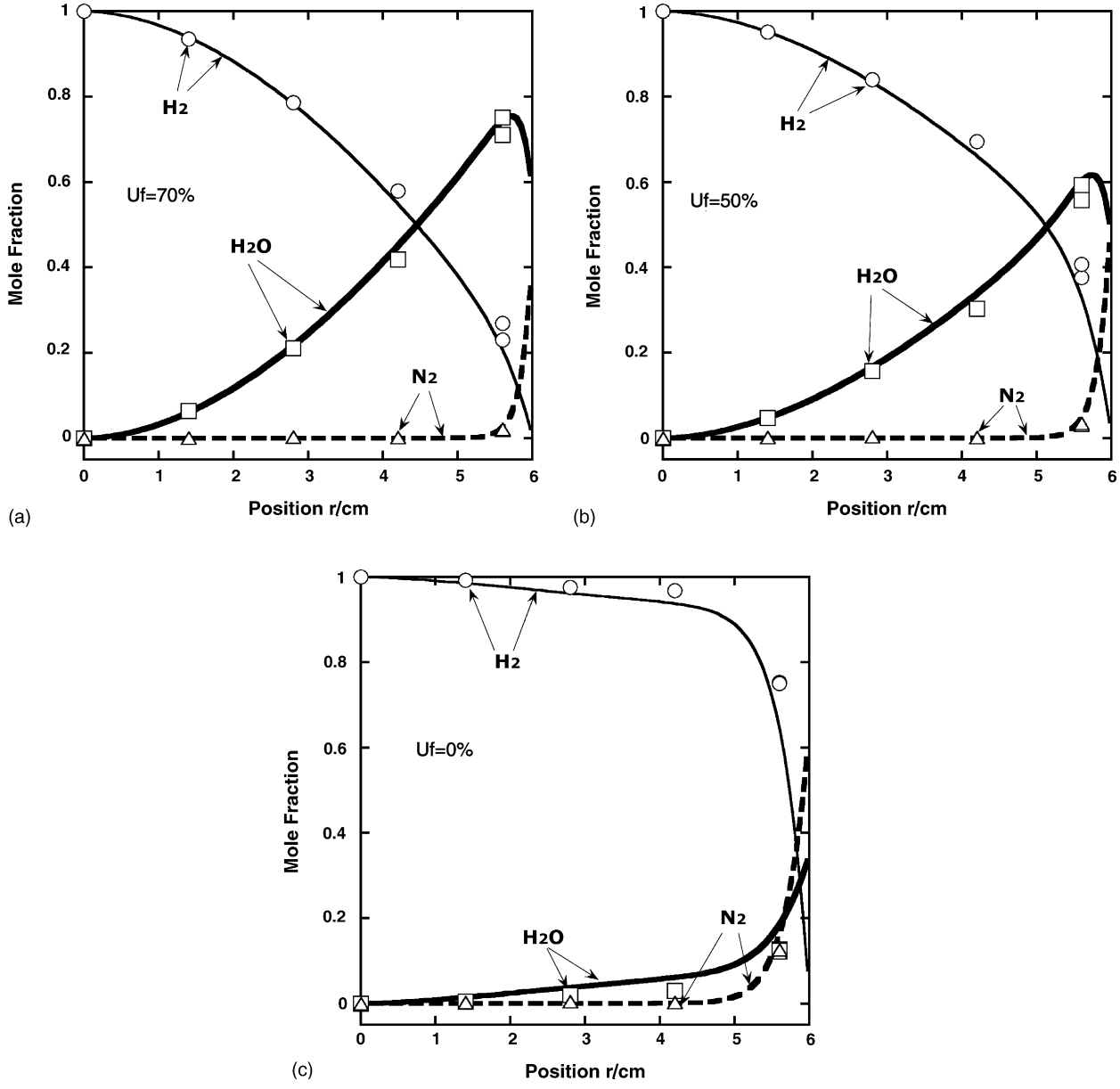

Fig. 9. Measured concentration (symbols) of H_2, H_2O and N_2 with the simulated profiles considering the back diffusion with doubled gas flow rate under: (a) $U_f = 70\%$, (b) $U_f = 50\%$ and (c) $U_f = 0\%$. 1023 K, H_2: 680 Ncc min^{-1}, air: 3400 Ncc min^{-1}.

under this assumption. The comparison of the experimental data of the three conditions reveals the abundance of N_2 back diffusion under less fuel utilization condition, which is obviously attributable to the superior diffusivity of N_2 in H_2 than in H_2O.

It is also suggested by the simulation that when the fuel utilization is small, for instance, at OCV (Fig. 7(c)), there appears minus current in the outermost region. This means that even when the output current is zero there is internal circulation current in the cell and hence, in the center region, fuel cell reaction is taking place, while at the outermost region, electrolysis reaction is expected to be taking place.

In Fig. 8, the observed *V–i* curve is plotted with the calculated one. They show quite good agreement with each other with only slight deviations at OCV and large current regions. The deviations can be explained as follows. When the current density is small, as was discussed, the internal circulation current appears and the opposite current (electrolysis current) was shown to be maximum at the outermost edge. However, in the practical situation, the outermost edge of the anode is not in fully reducing atmosphere because of the back diffusion and the anode in this region is in oxidizing condition. This has been confirmed by the post-experiment observation of the cell. Therefore, the anode in the outermost region, in which the largest opposite current is supposed to be flowing, is not working. This means, in reality, the internal circulation current is smaller than the estimated one and hence the cell voltage is larger than the calculated one.

The deviation, when the current density is large, is expected to appear as a result of the concentration polarization. Because we have estimated that the effect of the concentration polarization is not significant, the concentration polarization is not considered in the simulation. The small deviation between experimental data and the calculation in the large current density region, in turn, suggests the minor effect of the concentration polarization.

In this paper, the electronic transference number of the solid electrolyte is assumed to be 0.7%, taken as the optimum value to coincide the simulation with the experiment. The value, however, is little less than the value (1.5%), which is estimated by the comparison of the simulation and the experiment of ac impedance figures [9]. The discrepancy between the values is caused by the fact that the former impedance calculation did not take the effect of the back diffusion into account. The little larger electronic conduction estimated compensated the back diffusion, because both the electronic conduction in the electrolyte and the back diffusion work to make the cell voltage lower.

4.3. Compositional measurement and simulation under doubled gas flow rate

Compositional analyses were again conducted with the double gas flow rate, i.e., $H_2 = 680\ \mathrm{Ncc\ min^{-1}}$ and air = 3400 Ncc $\mathrm{min^{-1}}$. The data obtained using the same sampling ports as was mentioned are plotted with the simulated curves in Fig. 9(a) $U_f = 70\%$, (b) $U_f = 50\%$ and (c) at OCV. The general characteristics of the concentration profiles of the gaseous species do not differ much from the ones observed under the standard gas flow rate conditions (Fig. 7). The most remarkable difference between the two conditions is the concentration of N_2 at $r = 56$ mm. Because under the doubled flow rate, the flow speed of the gas (cm $\mathrm{s^{-1}}$) becomes consequently doubled, N_2 diffuses into the anode less easily.

Another noticeable difference between the two conditions, when compared at the same position, is that the concentration of H_2 becomes larger when the gas flow rate was doubled, and accordingly, the concentration of H_2O becomes less. This is because the relative amount of the consumption of H_2 owing to the internal leakage current becomes less when the gas flow rate increases.

It is also noticeable that the calculated concentrations of H_2O exceed those measured and the measured concentrations of H_2 exceed those calculated at the outlet region. This is presumably because our assumption of the complete oxidation of outlet H_2 at $r = 60$ mm no more applies to the condition where the gas flow rate becomes large. In this case, in the calculation, the situation could be expediently treated as that the complete oxidation takes place at $r > 60$ mm. Simple modification of the boundary condition has been tried and resulted in the partial explanation of the difference between the calculated concentrations and those measured of H_2, H_2O and N_2 in the outlet region.

The significantly suppressed back diffusion of N_2 in the outlet region under the increased gas flow rate discussed earlier works to make the cell voltage higher. The measured OCV at the standard gas flow rate was 1.026 V, while that at the doubled flow rate was 1.074 V. In the difference between

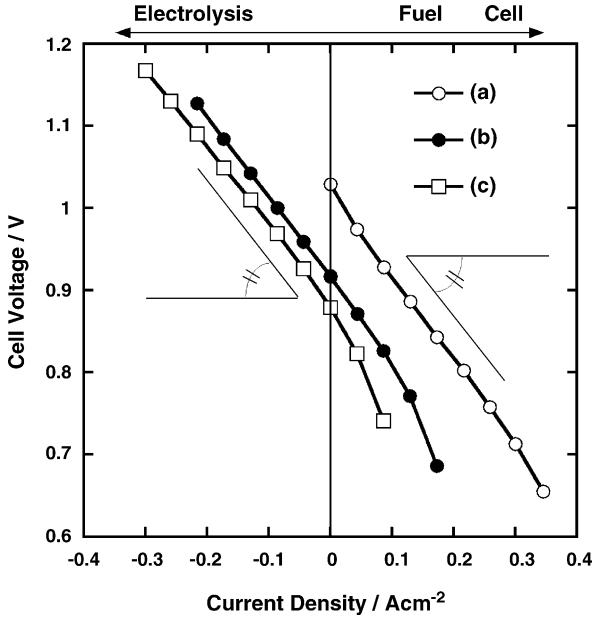

Fig. 10. Comparison of *V–i* characteristics under various conditions. Input anode gas compositions are: (a) H_2: 100%, (b) H_2: 50%, H_2O: 50% and (c) H_2: 30%, H_2O: 70%.

these OCVs, the effect of the difference in the relative amount of leakage owing to the electronic conduction is included as well as the effect, which comes from the difference in the back diffusion. Moreover, the comparison of the cell voltage under dc current with electronic conduction in the electrolyte is rather complicated because the effects of the overpotential and of the internal leakage current differ under different gas flow rate. Hence, the calculation was made as regard to OCVs assuming zero electronic conduction in the electrolyte. The result is that the doubled gas flow rate from 340 Ncc min^{-1} to 680 Ncc min^{-1} increases the OCV by about 40 mV, which is close to the observed difference, mostly owing to the effect of suppressed back diffusion of N_2 and H_2O.

4.4. Behavior under electrolysis operation

As has been shown by the simulation, the outermost region of the cell tends to work oppositely, i.e., toward electrolysis direction, especially when U_f is small. This is because the cell voltage exceeds the local emf in this region. The internal leakage current, the back diffusion and the upper stream cell current are responsible for this inversion. In the simulation, as was mentioned, the local cell resistance is assumed to be uniform throughout the cell. This means that the local cell resistance for the electrolysis reaction was assumed to be the same as for the fuel cell reaction. The assumption has to be checked, because the asymmetrical behavior of (fuel

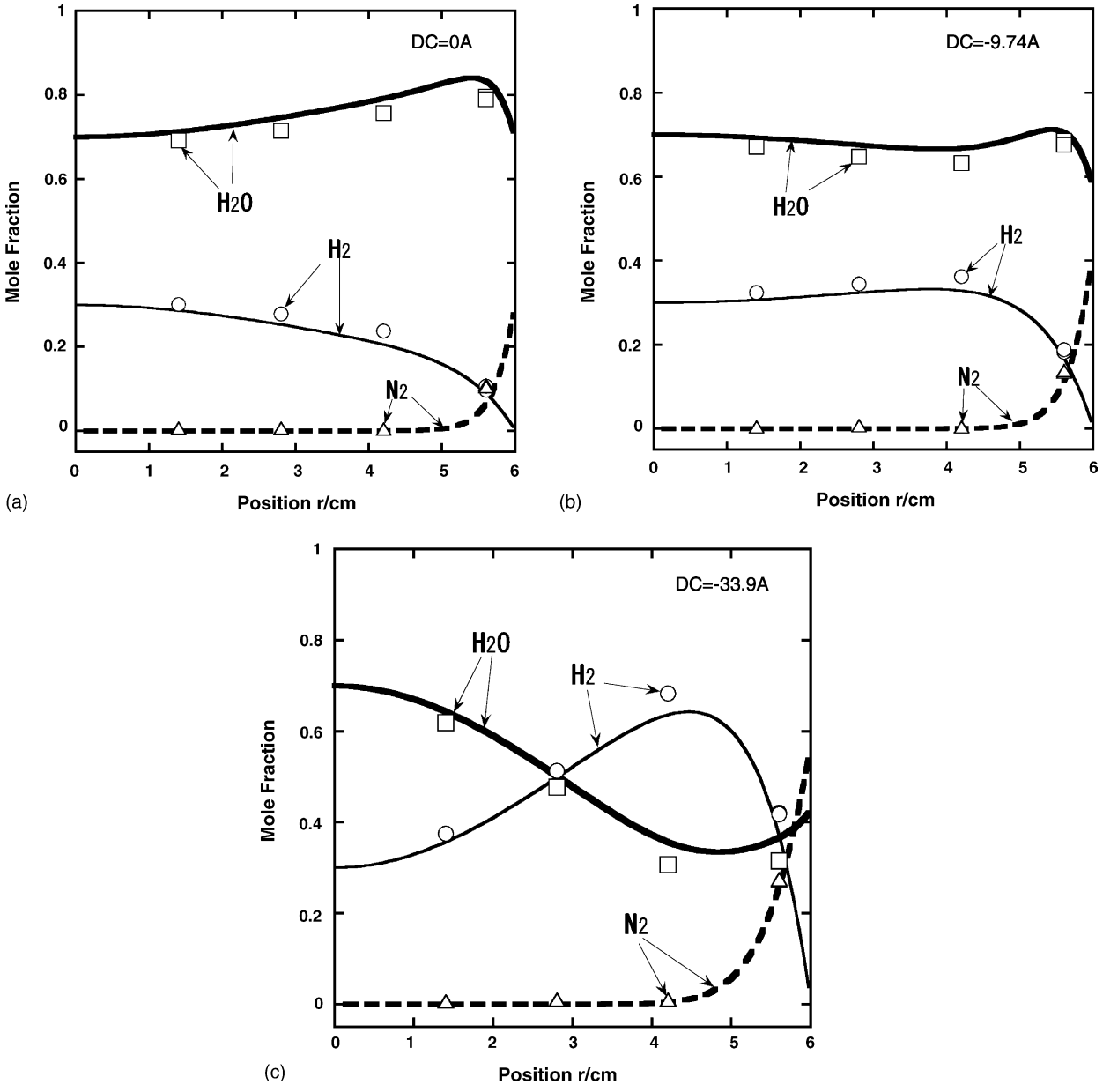

Fig. 11. Measured concentration (symbols) of H_2, H_2O and N_2 with the simulated profiles considering the back diffusion under electrolysis operation. Anode gas was supplied as a mixture of H_2 (30%, 103 Ncc min^{-1}) and H_2O (70%, 238 Ncc min^{-1}): (a) dc = 0 A, (b) dc = −9.74 A and (c) dc = −33.9 A. 1023 K, air: 1700 Ncc min^{-1}.

cell/electrolysis cell) directions is quite probable [10]. *V–i* curves were then taken under various input anode gas conditions for both directions and are shown in Fig. 10. Excluding the behaviors around the end points, where the abrupt change in Nernst loss occurs, the slops for both directions were found to be almost the same. Supplementary impedance measurements were also conducted under electrolysis conditions, but no significant difference in the resistances shown in Fig. 4 was found between the two directions.

The next experiment needed to confirm the assumption is to investigate whether hydrogen is really being produced or not with the reverse current, i.e., it is necessary to confirm that the current is used for the hydrogen production and not for the decomposition of the electrolyte, etc. For this purpose, the compositional measurements were again conducted under the electrolysis conditions and the results are plotted in Fig. 11 along with the simulated profiles. In the experiment, 30% H_2 and 70% H_2O mixture was supplied to the cell. In Fig. 11(c), the measurements were carried out under dc current of −33.9 A which corresponds to the exact amount of H_2O supplied to the anode, i.e., the same but opposite direction as for the fuel cell experiments with $U_f = 70\%$. Although there is some deviation between the observed data and the calculation, it is quite clear that hydrogen is being produced by the reverse current consuming H_2O. The deviation could also be made less assuming the non-conductive region at the outlet area as is discussed earlier in the Section 4.2.

Slight degradation in *V–i* characteristics was observed during the electrolysis measurements. The degradation is presumably attributable to the concentrated electrolysis current at the central region because the degradation characteristics of electrolysis cell tend to be strongly dependent on the polarization at the electrode and hence on the current density [10].

Overall, it was confirmed that these assumptions made in the simulation were reasonable enough to discuss the cell behavior observed here with some minor modifications if any.

5. Conclusions

The concentration measurement of the anode using practical SOFC was carried out. Simulations with and without considering the diffusion from the seal-less edge were also made and the following feature was clarified.

(1) The radial anode gas flow in the present cell was proved to be uniform within the error included in the measurement and the validity of the assumption for the simulation was shown.
(2) The comparison of the concentration data and the simulation indicated the existence of the back diffusion of N_2 and H_2O. It was also suggested that the diffusion reaches only slightly inside toward the center of the cell.
(3) The amount of the N_2 diffused into the anode increases with decreasing U_f because of the larger diffusion coefficient in H_2 than in H_2O.
(4) The existence of the electrolysis current inside the cell, especially when U_f is small, was predicted by the simulation. The electrolysis reaction was also shown to be possible with the present cell.
(5) The amount of the back diffusion of N_2 and H_2O decreases with increasing input gas flow rate and it was concluded that the depressed diffusion of N_2 and H_2O works to make the cell voltage higher.
(6) The simulated *V–i* curve almost coincides with the experiment, indicating the non-significance of the concentration polarization over the current density region investigated.

References

[1] M. Dokiya, M. Ubukata, T. Kikuchi, L. Nguyen, T. Kato, I. Anzai, in: S.C. Singhal, M. Dokiya (Eds.), Proceedings of the International Symposium on Solid Oxide Fuel Cells VIII, 2003-07, 2003, pp. 1260–1265.
[2] T. Kato, A. Negishi, L. Nguyen, K. Kato, K. Nozaki, T. Honda, K. Takano, A. Momma, Y. Kaga, M. Dokiya, Proc. Fuel Cell Semin. (2003) 303–306.
[3] M.C. S Williams, in: U. Stimming, S.C. Singhal, H. Tagawa, W. Lehnert (Eds.), Proceedings of the International Symposium on Solid Oxide Fuel Cells V, 97-40, 1997, pp. 3–11.
[4] K. Takano, S. Nagata, K. Nozaki, A. Momma, T. Kato, Y. Kaga, A. Negishi, K. Kato, T. Inagaki, H. Yoshida, K. Hosoi, K. Hoshino, T. Akbay, J. Akikusa, J. Power Sources 132 (2004) 42–51.
[5] T. Kato, K. Nozaki, A. Negishi, K. Kato, A. Momma, Y. Kaga, S. Nagata, K. Takano, T. Inagaki, H. Yoshida, K. Hosoi, K. Hoshino, T. Akbay, J. Akikusa, J. Power Sources 133 (2004) 169–174.
[6] J. Akikusa, T. Yamada, K. Adachi, K. Hoshino, T. Ishihara, Y. Takita, in: H. Yokokawa, S.C. Singhal (Eds.), Proceedings of the International Symposium on Solid Oxide Fuel Cells VII, 2001-16, 2001, pp. 159–165.
[7] K. Kuroda, I. Hashimoto, K. Adachi, J. Akikusa, Y. Tamou, N. Komada, T. Ishihara, Y. Takita, Solid State Ionics 132 (2000) 199–208.
[8] A. Momma, T. Kato, K. Nozaki, A. Negishi, K. Kato, Y. Kaga, S. Nagata, K. Takano, T. Inagaki, H. Yoshida, K. Hosoi, K. Hoshino, T. Akbay, J. Akikusa, in: S.C. Singhal, M. Dokiya (Eds.), Proceedings of the International Symposium on Solid Oxide Fuel Cells VIII, 2003-07, 2003, pp. 1186–1199.
[9] A. Momma, Y. Kaga, K. Takano, K. Nozaki, A. Negishi, K. Kato, T. Kato, T. Inagaki, H. Yoshida, K. Hosoi, K. Hoshino, T. Akbay, J. Akikusa, M. Yamada, N. Chitose, Solid State Ionics, 174 (2004) 87–95.
[10] A. Momma, T. Kato, Y. Kaga, S. Nagata, J. Ceram. Soc. Japan 105 (1997) 369–373.